JOC Article

A Simple and Efficient Route to N-Functionalized Dithieno[3,2-*b*:2′,3′-*d*]pyrroles: Fused-Ring Building Blocks for New Conjugated Polymeric Systems

Katsu Ogawa and Seth C. Rasmussen*

Department of Chemistry, North Dakota State University, Fargo, North Dakota 58105-5516

seth.rasmussen@ndsu.nodak.edu

Received January 22, 2003

A general synthetic route has been developed for the simple and efficient preparation of N-functionalized dithieno[3,2-*b*:2′,3′-*d*]pyrroles. These synthetic methods utilize N-functionalized *N*-(3′-thienyl)-3-aminothiophenes produced from the Pd-catalyzed amination of 3-bromothiophene with primary amines, followed by a one-pot bromination/cyclization process. This combination allows the convenient preparation of a variety of N-functionalized dithieno[3,2-*b*:2′,3′-*d*]pyrroles (where substituent = hexyl, octyl, decyl, *tert*-butyl, and *p*-hexylphenyl) in good yield (65−82%). Characterization of the structure and reactivity of this class of compounds is also described, including electrochemical and photophysical data for all compounds and X-ray structural data for the octyl-, *tert*-butyl-, and *p*-hexylphenyl-functionalized compounds.

Introduction

The optical and electronic properties of conjugated organic polymers are of considerable fundamental and technological interest. The importance of these materials was recently recognized with the awarding of the 2000 Nobel prize in chemistry to Alan J. Heeger, Alan G. MacDiarmid, and Hideki Shirakawa for the discovery and development of conjugated polymers.[1] Applications demonstrated for these materials include their use in batteries, sensors, electrochromic devices, light-emitting diodes, and field effect transistors.[2−6]

A potential advantage of utilizing conjugated polymers in such applications is the ability to tune the properties of the polymer at the molecular level. Tuning is typically accomplished through synthetic modification, which permits the incorporation of side-chain functionalities.[3−6] The ability to modify these properties is of the utmost importance for the efficient application of these materials. Soluble, stable systems are required for their processing, and the desirable properties of these polymers are dependent on the extent of conjugation. Increased conjugation lowers the band gap and results in an enhancement of the thermal population of the conduction band, thus increasing the number of intrinsic charge carriers. In addition, the lower oxidation potential associated with narrow band gaps results in a stabilization of the corresponding doped (i.e., oxidized) state.[7] Thus, the ability to sufficiently control such polymer properties is the key to the production of technologically useful materials.

Another approach to tuning the polymer properties is the annulation of aromatic rings to the repeat units. The use of such fused-ring precursors has been found to be a powerful approach to the production of low band gap, conjugated polymers. The first such example was polymers of isothianaphthene (**1**, Chart 1) which exhibit band gaps of 1.0−1.2 eV, approximately 1 eV lower than polythiophene.[7,8] The results obtained with poly(isothianaphthene) and its derivatives then led to interest in other fused-ring systems as potential precursors, as shown in Chart 1. In particular, various thieno[3,4-*b*]-pyrazines[9,10] (**2**), thieno[3,4-*b*]thiophene[11] (**3**), [1,2,5]thiadiazolo[3,4-*b*]thieno[3,4-*e*]pyrazine[12] (**4**), thieno[2,3-*b*]-

(1) The Nobel Foundation: http://www.nobel.se/chemistry/laureates/2000.

(2) (a) *Conjugated Conducting Polymers*; Kiess, H., Ed.; Springer Series in Solid State Sciences; Springer-Verlag: New York, 1992; Vol. 102. (b) Kaner, R. B.; MacDiarmid, A. G. *Sci. Am.* **1988**, *258* (2), 106. (c) Yam, P. *Sci. Am.* **1995**, *271* (1), 82.

(3) Baker, G. L. In *Electronic and Photonic Application of Polymers*; Bowden, M. J., Turner, S. R., Eds.; ACS Advances in Chemistry Series 210; American Chemical Society: Washington, DC, 1985.

(4) Tourillion, G. Polythiophene and its Derivatives. In *Handbook of Conducting Polymers*; Skothem, T. A., Ed.; Marcel Dekker: New York, 1986.

(5) (a) Roncali, J. *Chem. Rev.* **1992**, *92*, 711. (b) Schopf, G.; Kossmehl, G. *Adv. Polym. Sci.* **1997**, *129*, 1. (c) Leclerc, M.; Faid, K. *Adv. Mater.* **1997**, *9*, 1087. (d) Garnier, J. *Angew. Chem., Int. Ed. Engl.* **1989**, *28*, 513.

(6) Rasmussen, S. C.; Straw, B. D.; Hutchison, J. E. In *Semiconducting Polymers: Applications, Synthesis, and Properties*; Hsieh, B. R., Wei, W., Galvin, M., Eds.; ACS Symposium Series 735; American Chemical Society: Washington, DC, 1999.

(7) (a) Roncali, J. *Chem. Rev.* **1997**, *97*, 173. (b) Pomerantz, M. In *Handbook of Conducting Polymers*, 2nd ed.; Skotheim, T. A., Elsenbaumer, R. L., Reynolds, J. R., Eds.; Marcel Dekker: New York, 1998; pp 277−309.

(8) (a) Wudl, F.; Kobayashi, M.; Heeger, A. J. *J. Org. Chem.* **1984**, *49*, 3382. (b) Kobayashi, M.; Colaneri, N.; Boysel, F.; Wudl, F.; Heeger, A. J. *J. Chem. Phys.* **1985**, *82*, 5717. (c) Colaneri, N.; Kobayashi, M.; Heeger, A. J.; Wudl, F. *Synth. Met.* **1986**, *14*, 45. (d) Ikenoue, Y.; Wudl, F.; Heeger, A. J. *Synth. Met.* **1991**, *40*, 1. (e) King, G.; Higgins, S. J. *J. Mater. Chem.* **1995**, *5*, 447.

(9) (a) Pomerantz, M.; Chaloner-Gill, B.; Harding, L. O.; Tseng, J. J.; Pomerantz, W. J. *J. Chem. Soc., Chem. Commun.* **1992**, 1672. (b) Kastner, J.; Kuzmany, H.; Vegh, D.; Landl, M.; Cuff, L.; Kertesz, M. *Synth. Met.* **1995**, *69*, 593. (c) Kastner, J.; Kuzmany, H.; Vegh, D.; Landl, M.; Cuff, L.; Kertesz, M. *Macromolecules* **1995**, *28*, 2922.

10.1021/jo034078k CCC: $25.00
Published on Web 03/08/2003

CHART 1. Fused-Ring Precursors for Conjugated Materials

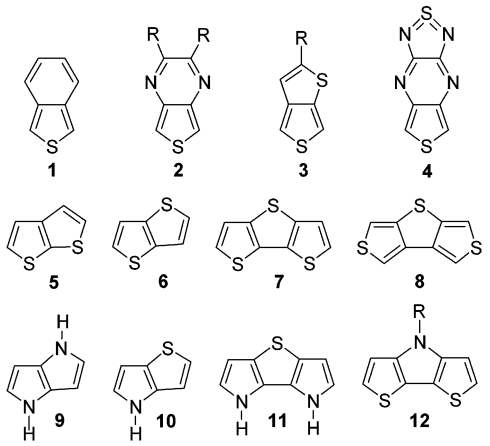

thiophene[13a] (**5**), thieno[3,2-*b*]thiophene[13b,c] (**6**), dithieno[3,2-*b*:2′,3′-*d*]thiophene[13a,c] (**7**), dithieno[3,4-*b*:2′,4′-*d*]thiophene[13d] (**8**), pyrrolo[3,2-*b*]pyrrole[14] (**9**), thieno[3,2-*b*]pyrrole[15] (**10**), dipyrrolo[3,2-*b*:2′,3′-*d*]thiophene[16a] (**11**), and dithieno[3,2-*b*:2′,3′-*d*]pyrroles[10c,16] (**12**) have all been investigated.[7]

While the use of fused-ring precursors can be an excellent approach to low band gap polymers, the synthesis of such precursors can be very laborious, especially if one wishes to incorporate side chains necessary for polymer solubility. Here we report the development of a new general synthetic route to N-functionalized dithieno-[3,2-*b*:2′,3′-*d*]pyrroles (**12**) which is both simple and efficient. This chemistry is an extension of our previously reported amination chemistry for the production of N-functionalized 3-aminothiophenes[17] combined with a new one-pot bromination/cyclization process that allows the production of the desired dithieno[3,2-*b*:2′,3′-*d*]pyrroles (DTPs) in high yields. This synthetic route allows convenient access to the desired long-chain alkyl functionalized precursors needed for the production of soluble poly(DTP)s and can be applied to the synthesis of a variety of N-functionalized DTPs. In addition, we include here the first full characterization of DTPs including the results of structural, electrochemical, and photophysical studies. Comparison of the resulting electronic and spectroscopic properties to known fused-ring thiophene and pyrrole compounds are also discussed in an attempt to better understand the structure−function relationships of such conjugated systems.

SCHEME 1. General Synthesis of N-Functionalized Dithieno[3,2-*b*:2′,3′-*d*]pyrroles

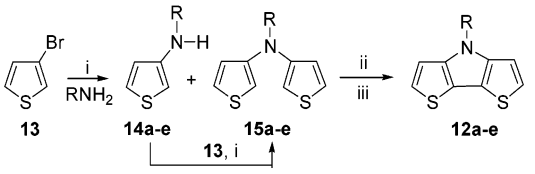

i. $Pd(OAc)_2/P(^tBu)_3$, NaO^tBu, xylene; ii. NBS, DMF; iii. Cu

a: R = C_6H_{13} **c**: R = $C_{10}H_{21}$ **e**: R = *p*-$C_6H_{13}Ph$
b: R = C_8H_{17} **d**: R = $C(CH_3)_3$

SCHEME 2. Previous Route to N-Functionalized Dithieno[3,2-*b*:2′,3′-*d*]pyrroles[16a,18]

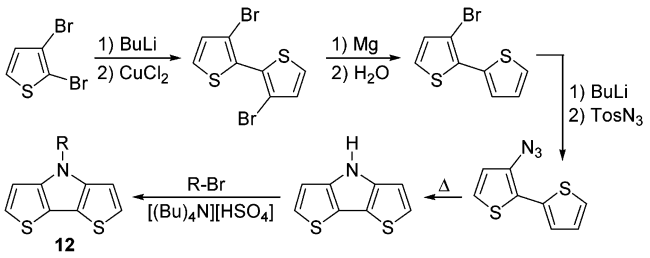

Results and Discussion

Synthesis. N-Functionalized DTPs can be readily synthesized directly from 3-bromothiophene as shown in Scheme 1.[17] In addition to its efficiency, this synthetic route allows the incorporation of a variety of functionizations by the simple selection of the primary amine reactant. The synthesis of the parent DTP was previously reported by Zanirato and co-workers in 1983.[18] Zotti and co-workers then extended this work by the addition of an alkylation step to produce the desired *N*-alkyl DTPs as shown in Scheme 2.[16a] Compared to this previous route, the newly presented methods (Scheme 1) reduced the total number of steps significantly and resulted in a 3-fold increase in the overall yields. In addition, while the initial thiophenes of both routes are commercially available, the 2,3-dibromothiophene used in Scheme 2 is approximately three times more expensive than the 3-bromothiophene used in the new methods.

As previously reported,[17] the initial amination of 3-bromothiophene (**13**) utilizing primary amines resulted in a mixture of N-functionalized 3-aminothiophenes (**14a**−**e**) and N-functionalized *N*-(3′-thienyl)-3-aminothiophenes (**15a**−**e**). However, these two components could easily be separated and further coupling chemistry with 3-bromothiophene converted the compounds **14a**−**e** to the analogous **15a**−**e** in high yield.

Initial attempts to convert tertiary amines **15a**−**e** to the desired DTPs **12a**−**e** utilized a modification of the methods of Wynberg and co-workers for the synthesis of cyclopentadithiophenones as shown in Scheme 3.[19] All attempts to isolate the intermediate products **16a**−**e**

(10) (a) Kenning, D. D.; Funfar, M. R.; Rasmussen, S. C. *Polym. Prepr.* **2001**, *42*, 506. (b) Kenning, D. D.; Mitchell, K. A.; Funfar, M. R.; Rasmussen, S. C. *Polym. Prepr.* **2001**, *42*, 665. (c) Kenning, D. D.; Ogawa, K.; Rothstein, S. D.; Rasmussen, S. C. *Polym. Mater. Sci. Eng.* **2002**, *86*, 59.

(11) Pomerantz, M.; Gu, X. *Synth. Met.* **1997**, *84*, 243.

(12) Tanaka, S.; Yamashita, Y. *Synth. Met.* **1997**, *84*, 229.

(13) (a) Jow, T. R.; Jen, K. Y.; Elsenbaumer, R. L.; Shacklette, L. W.; Angelopoulos, M.; Cava, M. P. *Synth. Met.* **1986**, *14*, 53. (b) Danieli, R.; Taliani, C.; Zamboni, R.; Giro, G.; Biserni, M.; Mastragostino, M.; Testoni, A. *Synth. Met.* **1986**, *13*, 325. (c) Taliani, C.; Zamboni, R.; Danieli, R.; Ostoja, P.; Porzio, W.; Lazzaroni, R.; Bredas, J. L. *Phys. Scr.* **1989**, *40*, 781. (d) Bolognesi, A.; Catellani, M.; Destri, S.; Porzio, W.; Taliani, C.; Zamboni, R. *Mol. Cryst. Liq. Crst.* **1990**, *187*, 519.

(14) Kumagai, T.; Tanaka, S.; Mukai, T. *Tetrahedron Lett.* **1984**, *25*, 5669.

(15) Lazzaroni, R.; Riga, J.; Verbist, J. J.; Christiaens, L.; Renson, M. *J. Chem. Soc., Chem. Commun.* **1985**, 999.

(16) (a) Berlin, A.; Pagani, G.; Zotti, G.; Schiavon, G. *Makromol. Chem.* **1992**, *193*, 399. (b) Pagani, G. A. *Heterocycles* **1994**, *37*, 2069.

(17) Ogawa, K.; Radke, K. R.; Rothstein, S. D.; Rasmussen, S. C. *J. Org. Chem.* **2001**, *66*, 9067.

(18) Zanirato, P.; Spagnolo, P.; Zanardi, G. *J. Chem. Soc., Perkin Trans. 1* **1983**, 2551.

(19) Jordens, P.; Rawson, G.; Wynberg, Hans, *J. Chem. Soc. C* **1970**, *2*, 273.

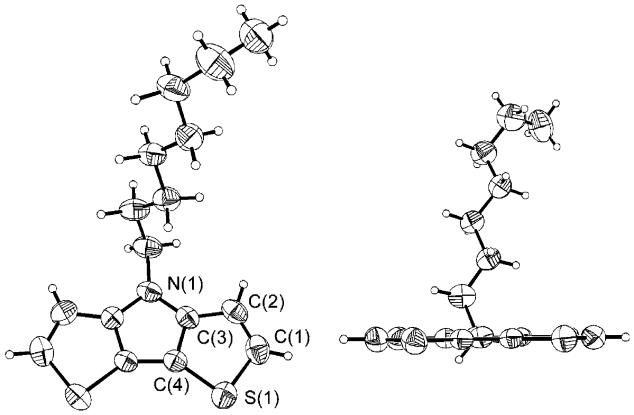

FIGURE 1. Face and edge ellipsoid plots of *N*-octyl DTP (**12b**).

SCHEME 3. Initially Proposed Cyclization Methods

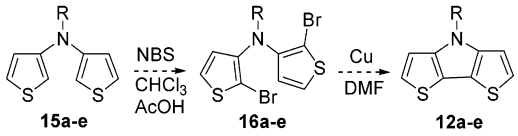

failed, however, due to the instability of these brominated compounds. Isolation attempts were made using either flash chromatography or distillation, but decomposition occurred in both processes. Even a quick filtration of the reaction mixture though a bed of silica gel would promote the decomposition of the desired intermediates.

Due to the observed instability of the brominated intermediates **16a**−**e**, a one-pot conversion of the compounds **15a**−**e** to the desired DTPs **12a**−**e** was then investigated. To accomplish this conversion without isolation of any intermediates, a solvent system compatible with both reactions needed to be found. As it was known that the copper chemistry worked well in DMF,[19] this was the first solvent investigated and such conditions were found to produce the desired DTPs in isolated yields of 65−82%. In attempts to optimize the yields of the DTP production, the bromination/cyclization reactions were also attempted in $CHCl_3$ and CH_3CN. While it is believed that bromination occurred in these solvents, cyclization failed to occur and no DTP products were observed.

X-ray Crystallography. Very little experimental data on the molecular geometry of compounds **1**−**12** have been reported and presently X-ray structural studies have only been carried out for **2** (R = CH_3)[20] and **6**.[21] It was found, however, that X-ray quality crystals of the DTPs could be grown by the slow evaporation of 2-propanol solutions, which allowed X-ray analyses to be performed on compounds **12b**,**d**,**e** as representative examples of the DTP series. The crystal structure of **12b** is shown in Figure 1 as an illustrative example. Selected bond angles and distances for these compounds, as well as for thiophene and pyrrole, are given in Table 1. The structures all show that the DTP fused-ring system is completely flat, with no bowing as is seen in some dibenzo-annulated thiophene and pyrrole compounds.[22] The flat nature of the DTP structure would then lead one to expect good conjugation across the π-system of the three rings.

TABLE 1. Experimental Geometrical Parameters of *N*-Octyl DTP (12b), *N*-*tert*-Butyl DTP (12d), *N*-(*p*-Hexylphenyl) DTP (12e), Thiophene, and Pyrrole

parameter	**12b**	**12d**	**12e**	thiophene[a]	pyrrole[a]
S(1)−C(1)	1.719	1.717	1.710	1.714	
S(1)−C(4)	1.717	1.716	1.708	1.714	
C(1)−C(2)	1.349	1.338	1.347	1.370	
C(2)−C(3)	1.417	1.428	1.416	1.423	
C(3)−C(4)	1.383	1.390	1.377	1.370	1.382
C(4)−C(4′)	1.420	1.406	1.422		1.417
N(1)−C(3)	1.380	1.385	1.390		1.370
C(1)−S(1)−C(4)	90.60	90.21	90.37	92.17	
S(1)−C(1)−C(2)	114.9	114.7	115.0	111.47	
S(1)−C(4)−C(3)	110.5	111.9	111.2	111.47	
C(1)−C(2)−C(3)	109.5	111.0	109.6	112.45	
C(2)−C(3)−C(4)	114.6	112.2	113.9	112.45	
C(3)−N(1)−C(3′)	106.7	106.0	105.9		109.8
N(1)−C(3)−C(4)	109.9	110.1	110.3		107.7
C(3)−C(4)−C(4′)	106.7	106.7	106.8		107.4

[a] Katritzky, A. R.; Pozharskii, A. F. *Handbook of Heterocyclic Chemistry*, 2nd ed.; Pergamon: New York, 2000; p 61.

Comparing the bond lengths of the DTPs with the experimental gas-phase distances of thiophene and pyrrole,[22] it can be seen that the annulation of the rings has resulted in deviations in both the pyrrole and thiophene portions of the DTP structure. Within the pyrrole portion, the greatest agreement with the parent structure is in the shared C═C bond between the two heterocyclic rings (i.e., C(3)−C(4) = 1.38−1.39 Å). As the analogous thiophene C═C bond is shorter in comparison to the pyrrole (1.370 vs 1.382 Å), it could be said that this shared bond is primarily pyrrole in character. Both of the remaining bonds within the pyrrole ring, however, exhibit elongation in comparison to the parent. In no case, though, does the length of the C(4)−C(4′) bond reach the 1.45 Å length of the interannular bond of 2,2′-bithiophenes,[23] implying that the central pyrrole ring does retain some aromatic nature. It is interesting to note, however, that compound **12d** differs from the other structures and actually shows a shortening of this C(4)−C(4′) bond. In fact, in **12d**, the three pyrrole bonds are much more equivalent, possibly indicating a greater aromatic nature to the pyrrole ring in comparison to the other DTPs.

While the central pyrrole is symmetrical in nature, the exterior thiophene rings show some asymmetry presumably due to the bond length mismatch between thiophene and pyrrole at the fused C(3)−C(4) bond. Thus, while the length of this bond matches well with the parent pyrrole, it is slightly elongated for the analogous bond in the parent thiophene. In contrast, however, the remaining C−C bonds of the thiophene rings are shortened in comparison to the parent thiophene. For example, in the most extreme case, the exterior C(1)−C(2) bond is shortened to approximately the same length as a typical simple C═C bond (1.34 Å).[24] While this could suggest a decrease in delocalization between this C═C and the rest

(20) Kenning, D. D.; Mitchell, K. A.; Calhoun, T. R.; Funfar, M. R.; Sattler, D. J.; Rasmussen, S. C. *J. Org. Chem.* **2002**, *67*, 9073.
(21) Cox, E. G.; Gillot, R. J. J. H.; Jeffrey, G. A. *Acta Crystallogr.* **1949**, *2*, 356.
(22) Katritzky, A. R.; Pozharskii, A. F. *Handbook of Heterocyclic Chemistry*, 2nd ed.; Pergamon: New York, 2000; pp 61, 80−81.
(23) Barbarella, G.; Zambianchi, M.; Antolini, L.; Folli, U.; Goldoni, F.; Iarossi, D.; Schenetti, L.; Bongini, A. *J. Chem. Soc., Perkin Trans. 2* **1995**, 1869.

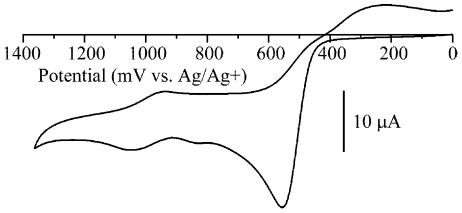

FIGURE 2. Cyclic voltammogram of *N*-octyl DTP (**12b**).

of the π-system, the adjoining C(2)−C(3) bond is also shortened, rather than elongated as would be expected in a case of bond fixation. The S−C bonds are of approximate length to the comparable bonds in the parent thiophene, but again asymmetry is exhibited in that the exterior S(1)−C(1) bonds are all slightly longer than the interior S(1)−C(4) bonds.

The potential for additional conjugation exists in the case of DTP **12e**, as π-overlap of the *p*-hexylphenyl group with the DTP is also possible. However, the phenyl ring of **12e** is not coplanar with the DTP ring and has a dihedral angle of 46.3°. This lack of planarity is probably due to steric interactions between the phenyl hydrogens and the hydrogens at C(2) and C(2′) of the fused-ring system. The fact that the phenyl−N(1) bond length (1.417 Å) is only slightly longer than the N(1)−C(3) bond, however, does suggest some overlap between the two π-systems.

While the DTP crystallographic data represents the first structural report of a fused-thieno[3,2-*b*]pyrrole unit, the calculated structure of thieno[3,2-*b*]pyrrole (**10**) has been determined using the MNDO method.[25] The calculated structure of **10** exhibits some similarities with the DTP structures, such as the bond length of the shared C(3)−C(4) bond, which again seems to be dictated by the pyrrole ring over the thiophene ring. The calculated structure also exhibits the same type of asymmetry in the S−C bonds, with the exterior bonds slightly longer than the interior bonds. The structure of **10**, however, does not exhibit the bond shortening in the exterior C=C thiophene bond seen in the DTP structures, but is actually slightly elongated in comparison to the parent thiophene.

Electrochemistry. The electrochemistry of the prepared DTPs has been investigated, and a representative cyclic voltammogram is shown in Figure 2. The combined electrochemical data of the DTP series is given in Table 2.

All of the DTPs exhibit a well-defined, irreversible oxidation presumably corresponding to the formation of the radical cation. Scanning to higher positive potentials results in two consecutive broad oxidations for most of the DTPs. As can be seen in Figure 2, the second oxidation is quite weak, followed by a more intense and well-defined third oxidation. Since coupling of thiophene radical cations is rapid ($\tau < 10^{-5}$ s),[26] these additional broad waves most likely correspond to the oxidation of coupled products as opposed to further DTP oxidations. The peak potentials of the first oxidation all occur at

TABLE 2. Electrochemical Data for a Series of N-Functionalized DTPs[a]

R	$E_{ox}1$ (V)	$E_{ox}2$ (V)	$E_{ox}3$ (V)
H	0.57[b]		
C_6H_{13}	0.56	0.83	1.03
C_8H_{17}	0.56	0.84	1.04
$C_{10}H_{21}$	0.56	0.83	1.02
^{t}Bu	0.57	0.81	0.98
p-C_6H_{13}Ph	0.65		1.10

[a] All potentials vs Ag/Ag^+. Voltammetric data were measured in millimolar argon-sparged CH_3CN solutions with 0.10 M $TBAPF_6$ as supporting electrolyte. [b] Berlin, A.; Pagani, G.; Zotti, G.; Schiavon, G. *Makromol. Chem.* **1992**, *193*, 399. Adjusted for differences in reference electrode.

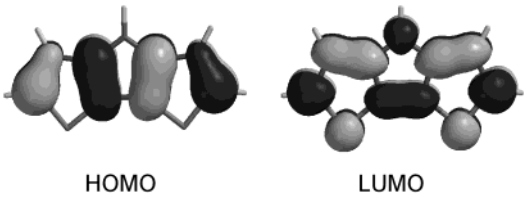

FIGURE 3. Calculated molecular orbitals of DTP.

approximately 0.56 V vs Ag/Ag^+, with the exception of **12e** which contains the conjugated *N*-phenyl ring. No reductions are observed upon scanning to negative potentials, but considering the energy of the lowest optical transition (see UV−vis Spectroscopy section), the first reduction should occur well outside the solvent window (∼−3.5 V).

The lack of influence of the simple alkyl substitutents on the oxidation potentials is consistent with previous studies on *N*-alkylpyrroles.[27] For simple pyrroles, *N*-alkylation is expected to impart little electronic perturbation to the pyrrole oxidation potential because these substituents exhibit weak electronic effects and reside at a node in the pyrrole HOMO. Thus, over a series of *N*-alkylpyrroles, changes of less than 60 mV have been seen between various alkyl substituents or the unfunctionalized parent pyrrole. As shown in Figure 3, the calculated HOMO of DTP[28] is similar to that of pyrrole and *N*-substituents also reside at a node in the DTP HOMO. In comparison to pyrroles, the DTP series shows even less deviation between the oxidation potentials of the *N*-alkyl DTPs and the unfunctionalized parent (∼10 mV or less).[16a]

For typical pyrroles, it is only when the N-substituents become either large or conjugated with the pyrrole that they can influence the redox potential of the pyrrole or impede the coupling of radical cations.[27] The influence of such groups in the DTPs, however, is greatly attenuated. For example, the addition of a *N*-*tert*-butyl group shifts the potential of pyrrole ∼100 mV more positive, but essentially has no effect in the analogous DTP **12d**. Likewise, *N*-phenylpyrrole undergoes oxidation 600 mV more positive than pyrrole, while **12e** exhibits a shift of

(24) *CRC Handbook of Chemistry and Physics*; Lide, D. R., Frederikse, H. P. R., Eds.; CRC Press: Boca Raton, FL, 1995; p 9-4.
(25) Buemi, G. *J. Chim. Phys. Phys.-Chim. Biol.* **1987**, *84*, 1147.
(26) Audebert, P.; Hapiot, P. *Synth. Met.* **1995**, *75*, 95.

(27) (a) Diaz, A. F.; Castillo, J.; Kanazawa, K. K.; Logan, J. A.; Salmon, M.; Fajardo, O. *J. Electroanal. Chem.* **1982**, *133*, 233. (b) Ferraris, J. P.; Guerrero, D. J. In *Handbook of Conducting Polymers*, 2nd ed.; Skotheim, T. A., Elsenbaumer, R. L., Reynolds, J. R., Eds.; Marcel Dekker: New York, 1998; pp 259−76.
(28) Calculations were performed using SPARTAN (Wavefunction, Inc.) by ab initio (HF STO-3G) methods.

TABLE 3. Electrochemical Data for a Series of Thiophene and Pyrrole Fused-Ring Heterocycles[a]

no. of rings	compd	E_{ox} (V)	compd	E_{ox} (V)	compd	E_{ox} (V)
1	thiophene	2.06[b]	pyrrole	1.20[b]		
2	**6**	1.40[c]	**9**	0.48[d]	**10**	0.90[e,f]
3	**7**	1.20[c]	**17**		**12**/**11**	0.85[f]/0.42[f,g]

[a] All potentials vs SCE. [b] Waltman, R. J.; Bargon, J. *Can J. Chem.* **1986**, *64*, 76. [c] Taliani, C.; Danieli, R.; Zamboni, R. *Synth. Met.* **1987**, *18*, 177. [d] Kumagai, T.; Tanaka, S.; Mukai; T. *Tetrahedron Lett.* **1984**, *25*, 5669. [e] Lazzaroni, R.; Riga, J.; Verbist, J. J.; Christiaens, L.; Renson, M. *J. Chem. Soc., Chem. Commun.* **1985**, 999. [f] Adjusted from Ag/Ag$^+$. [g] Berlin, A.; Pagani, G.; Zotti, G.; Schiavon, G. *Makromol. Chem.* **1992**, *193*, 399.

only 80 mV in comparison to the parent DTP. In both of these cases, the attenuation of the functional group effect is due to the larger π system of the DTP in comparison to pyrrole, which reduces either the steric or electronic contribution of the substituent.

The oxidation potentials of various fused-ring species of thiophene and pyrrole are compared in Table 3. Comparison of the two parent heterocycles shows that the oxidation of pyrrole occurs at much lower positive potentials than thiophene. This is thought to be a direct consequence of the high polarity of the N−H bond, which tends to increase the electron density of the pyrrole ring and destabilize the pyrrole HOMO.[29] In both the homogeneous pyrrole and thiophene series (i.e., thiophene → **6** → **7**), the oxidation potentials decrease with increasing conjugation as one might expect. Comparing the two series, however, the decrease in potential is much more rapid in the pyrrole series and the oxidation potential of the most conjugated thiophene species, **7**, is essentially the same as the equally conjugated bithiophene.[27a]

The trends displayed in the thiophene and pyrrole series suggest that higher pyrrole content should result in the lowest potentials, and this trend is supported by the oxidation potential of the mixed thieno[3,2-*b*]pyrrole (**10**) which falls just below the average of the thienothiophene and pyrrolopyrrole analogues **6** and **9**. This result also agrees with reported theoretical calculations which predict that for the three fused-ring dimers, compound stability should increase and HOMO energy decrease in the order **9** → **10** → **6**.[25] Unfortunately, the oxidation potential of dipyrrolo[3,2-*b*:2′,3′-*d*]pyrrole[30] (**17**) has not been reported which would allow one to determine whether a similar trend is present in the fused-ring trimer series. However, comparing **10** to the mixed fused-ring trimers **11** and **12** shows that the additional pyrrole ring in **11** results in a much larger reduction in potential than the additional thiophene of DTP **12**. From the various trends discussed above, one could suggest that the oxidation of **17** should occur near 0 V.

UV−vis Spectroscopy. The UV−vis absorption data for DTPs **12a**−**e** are given in Table 4, and representative spectra of **12b** are shown in Figure 4. With the exception of **12e**, which contains the conjugated *N*-phenyl ring, the DTP series all exhibit two transitions at 310 and 298 nm, as well as a higher energy shoulder at 289 nm. Due to the close energetic spacing of these transitions, it is reasonable to assign these as various vibrational components of the same electronic transition. The extinction coefficients for these transitions fall roughly between 2 × 10^4 and 3 × 10^4 M^{-1} cm^{-1}, with corresponding oscillator strengths of approximately 0.50. These correspond to strongly allowed transitions, and are significantly more intense than the transitions of the two parent heterocycles.[31] Pyrrole ring n → π* transitions would not be expected as the nitrogen lone pair is involved in the π-bonding. Thus, since n → π* transitions have not been identified for thiophenes,[31] the observed DTP absorptions should correspond to π → π* transitions. Such an assignment also agrees with the calculated HOMO and LUMO shown in Figure 3.

As can be seen in Figure 4, the absorption spectra are very solvent independent, with large changes in solvent polarity resulting in only minor shifts of 2−3 nm. In

TABLE 4. UV−vis Absorption and Emission Data for a Series of N-Functionalized DTPs

R	λ_{max}[a] (nm)	ϵ[a] (M^{-1} cm^{-1})	f	λ_{max}[b] (nm)	Φ_F[b]
H[c]	300	18 000		337	7.7 × 10^{-5}
	290	22 000			
	280 (sh)	18 000			
	235	6200			
C_6H_{13}	310	26 900	0.5633	325	9.16 × 10^{-4}
	298	30 400			
	289 (sh)	25 400			
	241	4100			
C_8H_{17}	310	26 100	0.5412	324	1.05 × 10^{-3}
	298	29 300		324[d]	(7.78 × 10^{-4})[d]
	289 (sh)	24 200			
	241	5500			
$C_{10}H_{21}$	310	23 100	0.5271	325	1.15 × 10^{-3}
	298	26 300			
	289 (sh)	22 500			
^{t}Bu	309	20 400	0.4349	327	1.53 × 10^{-3}
	298	23 400			
	288 (sh)	19 500			
	241	3600			
p-C_6H_{13}Ph	310	42 400	0.4364	342	2.80 × 10^{-3}
	300	46 700		484[e]	
	293 (sh)	41 100			
	261	18 000			

[a] In CH_2Cl_2. [b] In EtOH at room temperature. [c] In CH_3CN. Fujitsuka, M; Sato, T.; Sezaki, F.; Tanaka, K.; Watanabe, A.; Ito, O. *J. Chem. Soc., Faraday Trans.* **1998**, *94*, 3331. [d] In CH_3CN. [e] Phosphorescence.

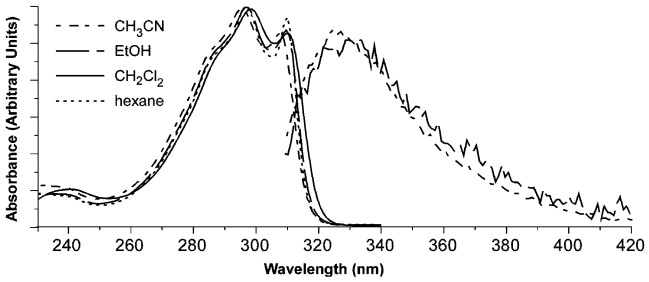

FIGURE 4. UV−vis and emission spectra of *N*-octyl DTP (**12b**).

(29) Gleiter, R.; Kobayshi, M.; Spanget-Larsen, J.; Gronowitz, S.; Konar, A.; Farnier, M. *J. Org. Chem.* **1977**, *42*, 2230.

(30) Aratani, T.; Yoshihara, H.; Suzukamo, G. *Tetrahedron Lett.* **1989**, *30*, 1655.

(31) Katritzky, A. R.; Pozharskii, A. F. *Handbook of Heterocyclic Chemistry*, 2nd ed.; Pergamon: New York, 2000; pp 68−9.

TABLE 5. UV−vis Absorption Data for a Series of Thiophene and Pyrrole Fused-Ring Heterocycles[a]

no. of rings	compd	λ_{max} (nm)	compd	λ_{max} (nm)	compd	λ_{max} (nm)
1	thiophene	231[b]	pyrrole	210[b]		
2	**6**	278[c]	**9**	245[e]	**10**	258[g]
3	**7**	298[d]	**17**	350[f]	**12**/**11**	310/282[h]

[a] In EtOH. [b] Katritzky, A. R.; Pozharskii, A. F. *Handbook of Heterocyclic Chemistry*, 2nd ed.; Pergamon: New York, 2000; p 68. [c] Brillante, A.; Samori, B.; Stremmenos, C.; Zanirato, P. *Mol. Cryst. Liq. Cryst.* **1983**, *100*, 263. [d] de Jong, F.; Janssen, M. *J. Org. Chem.* **1971**, *36*, 1645. [e] In cyclohexane. Kumagai, T.; Tanaka, S.; Mukai; T. *Tetrahedron Lett.* **1984**, *25*, 5669. [f] Aratani, T.; Yoshihara, H.; Suzukamo, G. *Tetrahedron Lett.* **1989**, *30*, 1655. [g] Soth, S.; Farnier, M.; Paulmier, C. *Can. J. Chem.* **1978**, *56*, 1429. [h] Farnier, M.; Soth, S.; Fournari, P. *Can. J. Chem.* **1976**, *54*, 1074.

comparison to the unfunctionalized parent DTP,[32] a small bathochromic shift is seen in the $\pi \rightarrow \pi^*$ transitions (∼8−10 nm). This is consistent with similar shifts seen upon *N*-functionalization of pyrroles,[33,34] and is reasonable considering that while the *N*-substituents reside at a node in the DTP HOMO, they do contribute to the DTP LUMO (Figure 3).

The lowest energy absorptions of various fused-ring species of thiophene and pyrrole are compared in Table 5. Comparison of the two parent heterocycles shows that the $\pi \rightarrow \pi^*$ transition of thiophene occurs at lower energy than pyrrole. In both the homogeneous pyrrole and thiophene series (i.e., thiophene → **6** → **7**), the $\pi \rightarrow \pi^*$ transitions shift to lower energy with increasing conjugation as one might expect. In addition, when comparing the two series, the red shift with each additional ring is greater for the thiophenes than for the pyrroles. The exception here is the extremely large shift between the pyrrole species **9** and **17** (∼105 nm). It is quite possible that the 350 nm value reported for dipyrrolo[3,2-*b*:2′,3′-*d*]pyrrole[30] (**17**) is in fact due to some oligomeric impurities resulting from the air oxidation of **17**. This is reasonable considering that, as previously discussed, the oxidation of **17** may occur near 0 V.

The trends displayed in the thiophene and pyrrole series would make it seem that higher thiophene content should result in the lowest energy transitions, and this trend is supported by the $\pi \rightarrow \pi^*$ transition of the mixed thieno[3,2-*b*]pyrrole (**10**) which falls just below the average of the thienothiophene and pyrrolopyrrole analogues **6** and **9**. Most interesting, however, are the trends seen in the mixed three-ring analogues **11** and **12**. Comparing these to the mixed bicyclic species **10**, both exhibit a red shift with the addition of the third fused ring as expected due to the increase in conjugation. However, the added thiophene ring results in a greater red shift than the addition of the pyrrole ring, consistent with the trends in the homogeneous series. The DTP **12** actually shows a slightly lower energy transition than the all thiophene analogue **7**, while the higher pyrrole content species **11** exhibits a transition slightly higher in energy than **7**.

Emission Spectroscopy. The fluorescence wavelengths and quantum yields (Φ_F) of **12a**−**e** are given in Table 4 and representative spectra of **12b** are shown in Figure 4. With the exception of **12e**, all of the DTPs studied exhibit a weak room temperature singlet emission at approximately 325 nm in ethanol. Excitation of all three major transitions resulted in the same emission profile and the excitation spectra show nearly equal contributions from all transitions. However, due to the weakness of the emission, solvent induced Raman scattering often overlapped the emission profile and it was found that only excitation at the high energy shoulder (289 nm) could produce a spectrum free of Raman scattering. The weak fluorescence of thiophene-based chromophores has been attributed to significant spin−orbit coupling.[32,35] This spin−orbit coupling is thought to be due to the heavy atom effect of the sulfur and is additionally mediated by charge transfer mixing, thus resulting in high triplet quantum yields (0.99 for bithiophene).[35] Highly efficient nonradiative processes between the triplet state and the ground state then leads to relaxation without emission. It is important to note, however, that phosphorescence was seen for the *N*-aryl DTP **12e** in addition to the fluorescence exhibited throughout the series. The phosphorescence maximum occurred at 484 nm and was approximately twice the intensity of the fluorescence maximum at 342 nm.

The fluorescence spectrum and quantum yield of the parent DTP was previously measured by Ito and co-workers in CH_3CN.[32] In comparison to the emission maxima of **12a**−**e**, the previously reported value was slightly lower in energy. While this difference could be attributed to solvent effects, the fluorescence of **12a**−**e** were relatively solvent independent. However, the fluorescence of the parent DTP may be more solvent dependent due to hydrogen bonding interactions between the solvent and the N−H bond of the DTP. The previously reported quantum yield (7.7×10^{-5}) was very low and almost an order of magnitude lower than the dithienothiophene analogue **7**. The authors attributed this lowered quantum yield of the DTP to a photochemical reaction with CH_3CN which reduced the yield of emission. In comparison, the measured quantum yields of **12a**−**e** are considerably greater and agree well with species **7**, even when the measurements were carried out in CH_3CN. As it was found that the emission intensities of **12a**−**e** were concentration dependent, it is believed that the lower quantum yields reported by Ito and co-workers were not the result of reaction with CH_3CN, but due to the fact that their measurements were carried out in relatively concentrated solutions (∼10^{-3} M) and thus were hindered by self-quenching.

Unfortunately, fluorescence lifetimes (τ_F) could not be measured for **12a**−**e** as the lifetimes were beyond the limits of detection (∼3 ns). From the measured oscillator strengths of the DTP series, a maximum radiative lifetime can be predicted using the relationship $k_e^0 = \nu_0^2 f$ (where ν_0 is the energy corresponding to the absorption maximum).[36] As the lifetime is $1/k_e$, this relationship gives a value of ∼2 ns for τ_F. However, this predicted value neglects alternate pathways to the ground state and thus the actual lifetime should be relatively smaller.

(32) Fujitsuka, M.; Sato, T.; Sezaki, F.; Tanaka, K.; Watanabe, A.; Ito, O. *J. Chem. Soc., Faraday Trans.* **1998**, *94*, 3331.
(33) Hinman, R. L.; Theodoropulos, S. *J. Org. Chem.* **1963**, *28*, 3052.
(34) Schofield, K. *Hetero-Aromatic Nitrogen Compounds. Pyrroles and Pyridines*; Plenum Press: New York, 1967; pp 51−58.
(35) Becker, R. S.; de Melo, J. S.; Macanita, A. L.; Elisei, F. *J. Phys. Chem.* **1996**, *100*, 18683.
(36) Turro, N. J. *Modern Molecular Photochemistry*; University Science Books: Sausalito, CA, 1991; pp 86−90.

Ito and co-workers, utilizing a picosecond system were also unable to determine a fluorescence lifetime due to the relatively weak emission.[32]

Conclusion

The newly reported synthetic route for N-functionalized DTPs is significantly more efficient than previous methods to these fused-ring species. These methods allow convenient access to the desired long-chain, alkyl-functionalized precursors needed for the production of soluble poly(DTPs) and can be applied to the synthesis of a variety of N-functionalized DTPs. In comparison, the incorporation of such functional groups into the majority of the fused-ring precursors **1**−**11** is not trivial. In addition, the resulting compounds **12a**−**e** are relatively stable and exhibit both low oxidation potentials and good conjugation, thus making them excellent building-blocks for conjugated polymeric systems. Comparison of the electronic and spectroscopic properties of the DTPs to known fused-ring thiophene and pyrrole compounds indicate that the pyrrole content seems to contribute to reduced oxidation potentials, while the thiophene content contributes to higher conjugation.

Experimental Methods

N-Functionalized *N*-(3′-thienyl)-3-aminothiophenes (**15a**−**e**) were prepared as previously reported.[17] Unless noted, all materials were reagent grade and used without further purification. Chromatographic separations were performed using standard column methods with silica gel (230−400 mesh). Dry DMF was obtained by treatment with $MgSO_4$ followed by distillation under reduced pressure. All glassware was oven-dried, assembled hot, and cooled under a dry nitrogen stream before use. Transfer of liquids was done by standard syringe techniques, and all reactions were performed under a stream of dry nitrogen.

Unless otherwise noted, the ^{1}H NMR and ^{13}C NMR spectra were carried out on a 300 MHz spectrometer. All NMR data was referenced to the chloroform signal and peak multiplicity was reported as follows: s = singlet, d = doublet, t = triplet, m = multiplet. Elemental analyses were performed in house.

General Procedure for Synthesis of N-Functionalized Dithieno[3,2-*b*:2′,3′-*d*]pyrroles (12a−e). The desired tertiary amine **15a**−**e** (10 mmol) was dissolved in 20 mL of dry DMF and cooled in an ice−water bath. Once the mixture had cooled, NBS (3.91 g, 22.0 mmol) in dry DMF (20 mL) was added dropwise over 2 h. Copper powder (0.95 g, 15 mmol) was then added and the reaction mixture heated under reflux for 2 h. The reaction was allowed to cool, filtered, and then extracted with hexanes (100 mL, 2 × 50 mL). The combined hexane washes were concentrated via rotary evaporation and purified by column chromatography (hexanes) to yield the product as a colorless oil that crystallized after cooling. Analytical samples were obtained by recrystallization from isopropyl alcohol.

***N*-Hexyldithieno[3,2-*b*:2′,3′-*d*]pyrrole (12a):** 68% yield; mp 41.7−42.5 °C; ^{1}H NMR ($CDCl_3$) δ 7.145 (d, J = 5.4 Hz, 2H), 7.020 (d, J = 5.4 Hz, 2H), 4.198 (t, J = 7.2 Hz, 2H), 1.874 (m, 2H), 1.316 (m, 6H), 0.890 (t, J = 6.9 Hz, 3H); ^{13}C NMR ($CDCl_3$) δ 145.19, 123.02, 114.83, 111.24, 47.68, 31.71, 30.63, 26.95, 22.80, 14.33. Anal. Calcd for $C_{14}H_{17}NS_2$: C, 63.83; H, 6.50; N, 5.32. Found: C, 63.54; H, 6.49; N, 5.06.

***N*-Octyldithieno[3,2-*b*:2′,3′-*d*]pyrrole (12b):** 65% yield; mp 34.6−35.2 °C; ^{1}H NMR ($CDCl_3$) δ 7.138 (d, J = 5.4 Hz, 2H), 7.012 (d, J = 5.4 Hz, 2H), 4.192 (t, J = 7.2 Hz, 2H), 1.868 (m, 2H), 1.253 (m, 10H), 0.885 (t, J = 6.9 Hz, 3H); ^{13}C NMR ($CDCl_3$) δ 145.21, 123.03, 114.85, 111.27, 47.68, 32.10, 30.68, 29.53, 29.45, 27.30, 22.94, 14.44. Anal. Calcd for $C_{16}H_{21}NS_2$: C, 65.93; H, 7.26; N, 4.81. Found: C, 65.94; H, 7.23; N, 4.84.

***N*-Decyldithieno[3,2-*b*:2′,3′-*d*]pyrrole (12c):** 66% yield; mp 31.2−32.0 °C; ^{1}H NMR ($CDCl_3$) δ 7.135 (d, J = 5.4 Hz, 2H), 7.009 (d, J = 5.4 Hz, 2H), 4.192 (t, J = 7.2 Hz, 2H), 1.864 (m, 2H), 1.243 (m, 14H), 0.886 (t, J = 6.9 Hz, 3H); ^{13}C NMR ($CDCl_3$) δ 145.16, 123.00, 114.80, 111.21, 47.67, 32.12, 30.63, 29.78, 29.72, 29.53, 29.51, 27.26, 22.94, 14.41. Anal. Calcd for $C_{18}H_{25}NS_2$: C, 67.66; H, 7.89; N, 4.38. Found: C, 67.68; H, 7.68; N, 4.17.

***N*-*tert*-Butyldithieno[3,2-*b*:2′,3′-*d*]pyrrole (12d):** 82% yield; mp 102.3−102.9 °C; ^{1}H NMR ($CDCl_3$) δ 7.245 (d, J = 5.4 Hz, 2H), 7.021 (d, J = 5.4 Hz, 2H), 1.823 (s, 9H); ^{13}C NMR ($CDCl_3$) δ 143.65, 122.20, 116.10, 115.12, 58.20, 30.93. Anal. Calcd for $C_{12}H_{13}NS_2$: C, 61.24; H, 5.57; N, 5.95. Found: C, 61.25; H, 5.57; N, 5.68.

***N*-(*p*-Hexylphenyl)dithieno[3,2-*b*:2′,3′-*d*]pyrrole (12e):** 66% yield; mp 57.4−58.0 °C; ^{1}H NMR ($CDCl_3$) δ 7.505 (d, J = 8.4 Hz, 2H), 7.342 (d, J = 8.4 Hz, 2H), 7.180 (s, 4H), 2.707 (t, J = 8.1 Hz, 2H), 1.713 (m, 2H), 1.400 (m, 6H), 0.964 (t, J = 6.9 Hz, 3H); ^{13}C NMR ($CDCl_3$) δ 144.34, 141.18, 137.77, 129.91, 123.56, 122.77, 116.87, 112.59, 35.82, 32.05, 31.81, 29.35, 22.96, 14.48. Anal. Calcd for $C_{20}H_{21}NS_2$: C, 70.75; H, 6.23; N, 4.13. Found: C, 70.74; H, 6.15; N, 3.91.

Crystallography. X-ray quality crystals of the DTPs were grown by the slow evaporation of 2-propanol solutions. The X-ray intensity data were measured at 298 K on a Bruker SMART 1000 CCD-based X-ray diffractometer system equipped with a Mo-target X-ray tube (λ = 0.710 73 Å) operated at 2000 W of power. The detector was placed at a distance of 5.047 cm from the crystal. A total of 1321 frames were collected with a scan width of 0.3° in ω and exposure time of 10 s/frame. The total data collection time was 3.7 h. The frames were integrated with the Bruker SAINT software package using a narrow-frame integration algorithm. All data were integrated using a triclinic unit cell and the structures were refined using the Bruker SHELXTL (Version 5.1) Software Package.

The final cell constants of **12b**: a = 13.089(2) Å, b = 9.3002(14) Å, c = 13.861(2) Å, β = 108.97(3)°, V = 1595.7(4) Å^3. **12d**: a = 12.8020(7) Å, b = 11.5375(7) Å, c = 17.6364(10) Å, β = 110.7740(10)°, V = 2435.6(2) Å^3; **12e**: a = 12.9396(12) Å, b = 7.9145(7) Å, c = 35.458(3) Å, β = 96.465(2)°, V = 3608.2(6) Å^3.

Electrochemistry. Cyclic voltammetry (CV) experiments were performed on a Bioanalytical Systems BAS 100B/W electrochemical analyzer. All measurements were made at a sweep rate of 100 mV/s. CVs were carried out in a three-electrode cell consisting of a platinum disk working electrode, a platinum wire auxiliary electrode, and a Ag/Ag^+ reference electrode (0.291 vs SCE).[37] Millimolar solutions of the samples were prepared by dissolution in CH_3CN dried over molecular sieves. The supporting electrolyte was 0.10 M tetrabutylammonium hexafluorophosphate ($TBAPF_6$). The solutions were deoxygenated by sparging with argon prior to each scan and blanketed with argon during the scans. The platinum disk working electrode was polished with 0.05 mm alumina and washed well with deionized water and dry CH_3CN prior to each scan.

Spectroscopy. UV−vis spectroscopy was performed on a dual-beam scanning UV−vis−NIR spectrophotometer using samples prepared as dilute CH_2Cl_2 or CH_3CN solutions in quartz cuvettes. Spectroscopy solvents were dried over molecular sieves prior to use. Oscillator strengths were calculated from the visible spectra using literature methods.[36] Emisson spectroscopy was performed using dilute solutions ($<10^{-5}$ M) at room temperature. Prior to each fluorescence measurement, the absorption spectrum was measured to ensure that the maximum absorption of the solution was less than 0.1. Samples were excited at 289 nm (296 nm for **12e**) and all spectra were obtained by averaging five scans. Quantum yields

(37) Larson, R. C.; Iwamoto, R. T.; Adams, R. N. *Anal. Chim. Acta* **1961**, *25*, 371.

were determined using secondary methods with anthracene as the reference.[38]

Acknowledgment. We thank the donors of the Petroleum Research Fund, administered by the American Chemical Society, for partial support of this research. Additional support was provided by North Dakota EPSCoR, the National Science Foundation (CHE-0132886), and North Dakota State University. We also thank Dean Grier for his assistance with the X-ray crystal analysis and Dr. Kenton R. Rodgers for his helpful discussions.

(38) (a) *Standards in Fluorescence Spectrometry*; Miller, J. N., Ed.; Chapman and Hall: New York, 1981; pp 68−78. (b) *Handbook of Organic Photochemistry*; Scaiano, J. C., Ed.; CRC Press: Boca Raton, FL, pp 233−236.

Supporting Information Available: IR and R_f data for compounds **12a**−**e**. Absorption and emission spectra of compound **12e**. Full crystallographic details and data for compounds **12b**,**d**,**e**. Electrochemical and UV−vis data for compounds **15a**−**e**. This material is available free of charge via the Internet at http://pubs.acs.org.

JO034078K